Construction and application of an electrochemical biosensor based on an endotoxin aptamer

GuoQing Ying[1,2]
MinJun Wang[2]
Yu Yi[2]
JianShu Chen[2]
JianFeng Mei[2]
YanLu Zhang[2]
ShuQing Chen[1*]

[1] College of Pharmaceutical Science, ZheJiang University, HangZhou, People's Republic of China

[2] College of Pharmaceutical Science, ZheJiang University of Technology, HangZhou, People's Republic of China

Abstract

An electrochemical biosensor that used an aptamer as a biological element was constructed to detect endotoxin. Biolayer interferometry was used to obtain the affinity constant of an aptamer for lipopolysaccharide, which had an equilibrium dissociation constant of 22.9 nM. The amine-terminated aptamer was then assembled on a gold electrode surface using 3-mercaptopropionic acid as an intermediate linker. The modification of the gold electrode was confirmed by cyclic voltammetry and electrochemical impedance spectroscopy. In the range of 0.001–1 EU/mL, the increase in electron transfer resistance of the biosensor was linear with the logarithmic value of the endotoxin concentration. The constructed biosensor exhibits sensitivity and a low limit of detection. Volume 00, Number 0, Pages 1–5, 2017

Keywords: *aptamer, biosensor, cyclic voltammetry, electrochemical impedance spectroscopy, electrochemistry, endotoxin*

1. Introduction

Endotoxin is a component of the Gram-negative bacterial cell wall and is toxic to the host. The main component of endotoxin is lipopolysaccharide (LPS), which is composed of three parts, O-antigen, core region, and lipid A. Lipid A is the main active ingredient of LPS, is a strong immune-stimulating factor, and can provide cell integrity and elicit an immune response in the host [1]. Because of its toxicity, it is important to detect and remove endotoxin in biological products [2]. The *limulus* test has been widely employed as a simple and sensitive method for the determination of endotoxin [3]. However, it has some shortcomings: The test results were susceptible to the color and turbidity of sample. In addition, the composition of *limulus* reagent is the blood of rare animal *Limulidae* does not meet the principle of sustainable development. A sensitive, convenient, environmentally friendly detection method is urgently needed and to be developed. With the rapid development of molecular biology and genetic engineering, especially the completion of the human genome project, research on nucleic acids has been expanding. Tuerk and Goldberg independently established nucleic acid libraries in 1990 [4], and these gradually developed into a nucleic acid library to screen ligand-efficient, specific combinations of DNA or RNA fragments using the index-rich ligand system evolution. Aptamers, in addition to their specificity and affinity, are characterized by their low molecular weight, numerous ligands, no immunogenicity, and *in vitro* selection independent of animals or cells [5]. As a result, aptamers are attractive for fabrication of aptamer-based biosensors.

Biosensors can be divided into two broad categories: those based on optical detection [6, 7] and those on electrochemical detection [8, 9]. Electrochemical analysis is widely used

Abbreviations: *BSA, bovine albumin; CV, cyclic voltammetry; EIS, electrochemical impedance spectroscopy; EDC, 1-(3-dimethylaminopropyl)-3-ethylcarbodiimide hydrochloride; LPS, lipopolysaccharide; MES, morpholinoethanesulfonic; MPA, 3-mercaptopropionic acid; NHS, N-hydroxysuccinimide; PBS, phosphate buffer solution; SELEX, systematic evolution of ligands by exponential enrichment.*

*Address for correspondence: ShuQing Chen, PhD, College of Pharmaceutical Science, ZheJiang University, HangZhou 310013, People's Republic of China. Tel: 0571-88320746; Fax: 0571-88871029; e-mail: chenshuqing@zju.edu.cn.

Received 23 May 2017; accepted 3 September 2017

DOI: 10.1002/bab.1610

Published online in Wiley Online Library (wileyonlinelibrary.com)

in biosensing as a sensitive, low-cost, simple, portable, and *in vivo* detection method. The construction of a new generation of aptamer electrochemical sensors has become an important research field that combines life sciences and analysis. Aptamer-based fluorescence sensors have been fabricated from a truncated progesterone (P4) aptamer that was highly selective for P4 [10]. A biosensor based on the electrochemical detection of endotoxin using a synthetic peptide assembled on a thin film has also been reported [11].

In our previous study, the aptamer EAQ3 was selected by SELEX [12]. In the present study, EAQ3, which has an equilibrium dissociation constant (K_D) of 22.9 nM and a high affinity for endotoxin, is detected by biolayer interferometry. We modified the 5′ end of this aptamer with amine groups. The amine-modified aptamer is then assembled on a gold electrode surface using 3-mercaptopropionic acid (MPA) as an intermediate linker. The constructed biosensor using cyclic voltammetry (CV) and electrochemical impedance spectroscopy (EIS) was used for characterization. This biosensor has the advantages of simple operation, low detection limit, and high sensitivity.

2. Materials and Methods

2.1. Materials

LPS from *Escherichia coli* 055: B5 (L2880) was purchased from Sigma-Aldrich (Saint Louis, MO, USA). Endotoxin from *E. coli* 0111:B4 was purchased from Chinese Horseshoe Crab Reagent Manufactory (Xiamen, People's Republic of China). The aptamer, biotin-labeled aptamer, and amino-modified aptamer were synthesized by Sangon (Shanghai, People's Republic of China) and purified by high-performance liquid chromatography. Morpholinoethanesulfonic acid (MES), *N*-hydroxysuccinimide (NHS), *N*-(3-dimethylaminopropyl)-*N*-ethylcarbodiimide hydrochloride (EDC), potassium ferricyanide ($K_3Fe(CN)_6$), and potassium hexacyanoferrate ($K_4Fe(CN)_6$) were purchased from Aladdin (China) and used without further purification. Other reagents were of analytical grade.

2.2. Determination of the affinity of aptamers for LPS by biolayer interferometry

The EAQ2 and EAQ3 aptamers were selected from an oligonucleotide library of 75 nucleotides using SELEX [13]. DNAMAN 8.0 was used to simulate their secondary structure. Both of them contained stem loops (Fig. 1). The affinity between two aptamers and LPS was determined by biolayer interferometry. Affinity measurements were conducted with an Octet K2 equipped with streptavidin (SA) biosensor tips (Pall-Fortebio, USA). The assays were performed at 30 °C and 503 ×*g*. The SA tips were loaded with 100 nM of the biotinylated aptamer for 100 Sec. The association rate constant (k_{on}) and dissociation rate constant (k_{dis}) of the reaction were then established by dipping the biosensors for 100 Sec in various concentrations of LPS in PBS (10 mM; pH 7.4; 40, 80, 160, and 320 nM). The data obtained were analyzed using Octet data analysis software version 9.0 (Forte Bio), and the obtained data were fitted with a 1: 1 combination model. K_D was calculated from $K_D = k_{dis}/k_{on}$ [14]. As shown in the following formula, which describes the equilibrium dissociation relationship between the aptamer and endotoxin, A represents a ligand assembled on the biosensor and B represents the analyte in solution:

$$A + B \underset{K_{on}/K_{dis}}{\longleftrightarrow} Complex$$

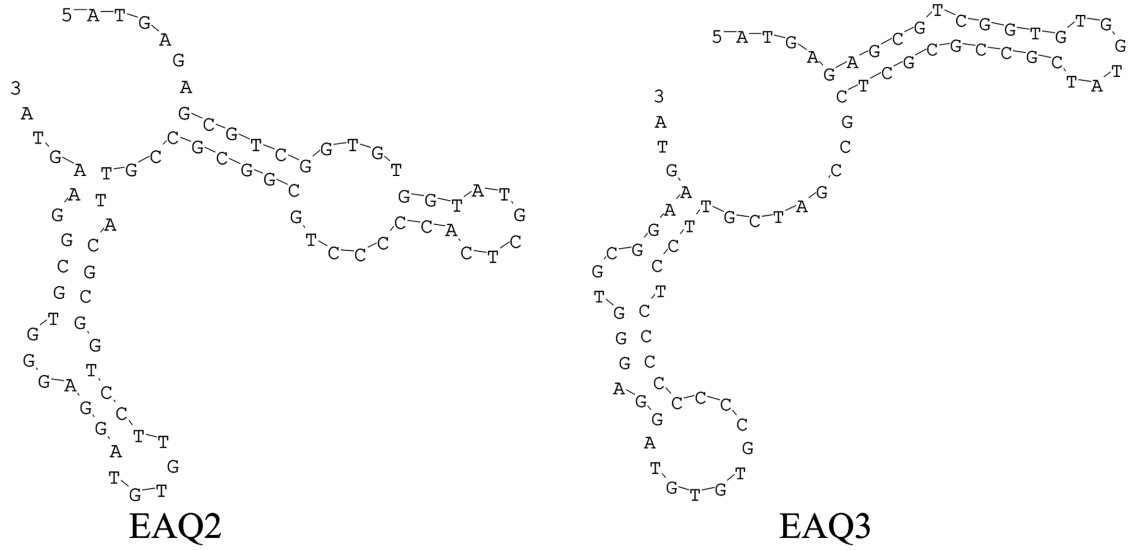

FIG. 1 *The simulation secondary structure of aptamers.*

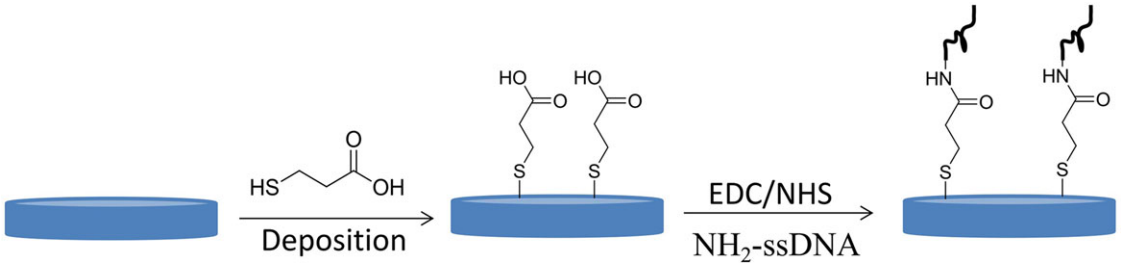

FIG. 2 *Stepwise construction of the biosensor.*

2.3. Construction of the biosensor

The gold electrode was electrolytically polished in 0.5 M H_2SO_4 by CV from 0 to 1.6 V at a scan rate of 100 mV Sec^{-1}. Afterwards, the electropolished electrode was immediately immersed in MPA in ethanol (200 mM) for 6 Hr. Residual MPA molecules were removed with absolute ethanol after self-assembly. The MPA-modified gold electrode was then immersed in 100 mM MES containing 20 mM EDC and 20 mM NHS for 1 Hr to activate the carboxyl groups of MPA [15]. Finally, the aptamer EAQ3 was assembled on the activated MPA-modified electrode by immersing the electrode in a 200 nM solution of the aptamer in phosphate-buffered saline (PBS; 10 mM, pH 7.4) for 1 Hr. This biosensor construction process is outlined in Fig. 2.

2.4. Application of the biosensor

The constructed biosensor was incubated in various concentrations of endotoxin solution in different environments at 25 °C for 40 Min. The electrode was then characterized by CV and EIS to characterize its change of resistance. All the materials used in these experiments were pyrogen-free.

3. Results and Discussion

3.1. Affinity of the aptamers for LPS

We used biolayer interferometry to measure aptamer–LPS interactions in real time using the SA-based sensors. The capture levels of the five SA sensors were in the range of 0.6–0.7 nm, indicating the sensors possess good binding affinity for the aptamers and can be used for subsequent LPS detection. We deducted data fitted according to a 1:1 combination model. The rate of EAQ2/EAQ3 binding to LPS was concentration dependent. We used these data to obtain the k_{on}, k_{dis}, and K_D values employing Octet software. Table 1 shows the k_{on}, k_{dis}, and K_D values for the two aptamers EAQ2 and EAQ3. The data reveal that although k_{dis} of EAQ2 is less than that of EAQ3, K_D of EAQ3 is almost twice that of EAQ2. In addition, we usually use $1/K_D$ to express affinity; the affinity of EAQ3 was significantly higher than that of EAQ2, so EAQ3 is a suitable biological component to detect LPS.

TABLE 1 ***Binding parameters of aptamers with LPS***

aptamer	K_{on} *(mSec^{-1})*	K_{dis} *(Sec^{-1})*	K_D *(M)*	R^2
EAQ2	3.82×10^4	1.24×10^{-3}	3.25×10^{-8}	0.9969
EAQ3	6.5×10^4	1.49×10^{-3}	2.29×10^{-8}	0.9944

The different concentrations of LPS as a set of data were analyzed to obtain K_{on} and K_{dis} data. K_D was calculated from $K_D = k_{dis}/k_{on}$.

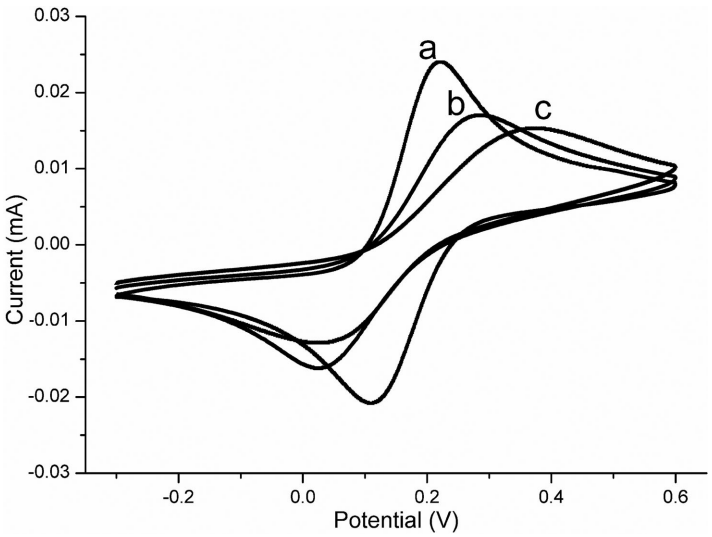

FIG. 3 *Cyclic voltammograms of the (a) bare gold electrode, (b) MPA-modified electrode, and (c) aptamer-immobilized electrode between −0.3 and 0.6 V in PBS (10 mM, pH 7.4) containing 2 mM $K_3Fe(CN)_6/K_4Fe(CN)_6$.*

3.2. Construction of the biosensor

During the construction of the biosensor, we characterized each step by CV and EIS. CV of $Fe(CN)_6^{3-/4-}$ in PBS (10 mM, pH 7.4) measured in the range of −0.3 to 0.6 V with a scan rate of 100 mV Sec^{-1} is presented in Fig. 3. The redox reaction between $K_3Fe(CN)_6$ and $K_4Fe(CN)_6$ on the surface of the bare gold electrode had redox peak potentials E_{pa} of 220 and 123

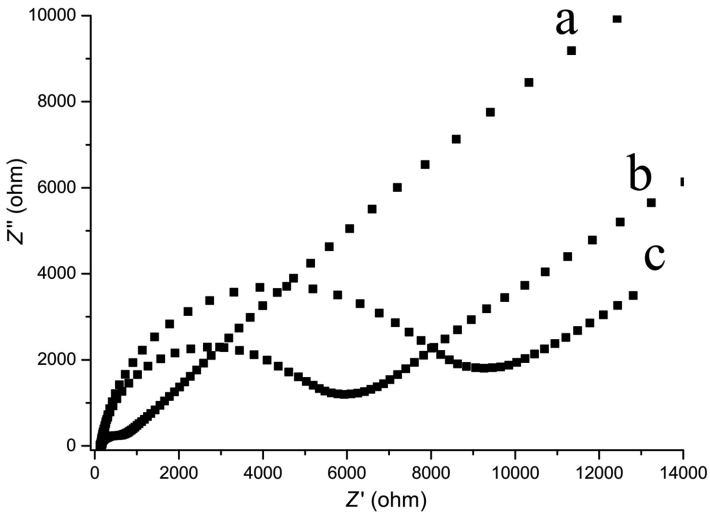

FIG. 4 *Nyquist plots of the various electrodes in PBS (10 mM, pH 7.4) containing 2 mM $K_3Fe(CN)_6/K_4Fe(CN)_6$: (a) bare gold electrode, (b) MPA-modified electrode, and (c) aptamer-immobilized electrode.*

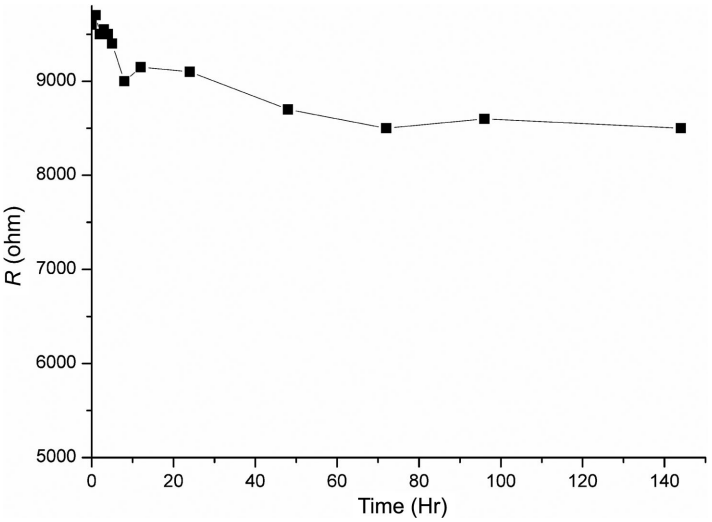

FIG. 5 *The stability of biosensor.*

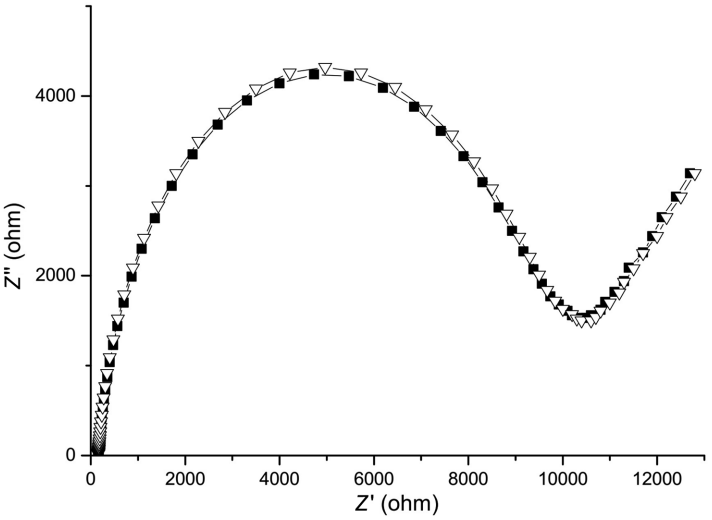

FIG. 6 *Nyquist plots of the biosensor incubating in endotoxin containing different concentration of BSA: (▽) containing 500 ng/ml BSA, (■) without BSA.*

mV, and peak current I_{pa} of 0.027 and 0.024 mA, respectively (ΔE_{pa} = 97 mV, $I_{pc}/I_{pa} \sim 1$), indicating that the oxidation and reduction of the $K_3Fe(CN)_6/K_4Fe(CN)_6$ pair was almost unimpeded on the unmodified gold electrode surface. In contrast, for the gold electrode modified with MPA in $K_3Fe(CN)_6/K_4Fe(CN)_6$ electrolyte, the potential difference and redox peak current decreased obviously compared with those for the unmodified electrode, indicating that MPA had self-assembled on the gold electrode surface. The MPA self-assembled monolayer could prevent the redox reaction of $K_3Fe(CN)_6/K_4Fe(CN)_6$ at the electrode surface [16]. After the electrode was exposed to the aptamer, the redox peak current decreased further, indicating that the aptamer was successfully fixed on the MPA-modified electrode surface. Because of a large number of electronegative phosphate groups in the aptamer, the electrolyte to the electrode surface was limited [17].

The EIS curves of the various gold electrodes in $K_3Fe(CN)_6/K_4Fe(CN)_6$ electrolyte are shown in Fig. 4. The Nyquist plots contain a semicircle at higher frequency and a linear region at lower frequency. The Nyquist plot of the bare gold electrode is almost a straight line, implying that the bare gold electrode has no effect on the redox reaction of $K_3Fe(CN)_6/K_4Fe(CN)_6$. The presence of an MPA SAM on the gold electrode caused a semicircle to appear in the Nyquist plot at high frequency. As mentioned above, an MPA SAM on the gold electrode surface could limit the redox reaction of $K_3Fe(CN)_6/K_4Fe(CN)_6$. When the aptamer was assembled on the gold electrode, a semicircle with a larger diameter appeared in the high-frequency region of its Nyquist plot, indicating an increase in impedance. As mentioned above, the negative charge of aptamers will hinder the contact between the redox probe and electrode surface and thus affect the electron transfer, resulting in increased resistance. In addition, the aptamer itself on the electrode surface has a large molecular weight and will also affect electron transfer. Both of the CV experiments and impedance results indicated that the biosensor can be constructed.

3.3. Application of the biosensor

The stability of the biosensor was examined before endotoxin detection. The biosensor was stored in the PBS (10 mM, pH 7.4) at 4 °C. The biosensor maintained a steady EIS response value after 1 week, and the response value still occupied 90% (Fig. 5); the stability of the biosensor is good. Since

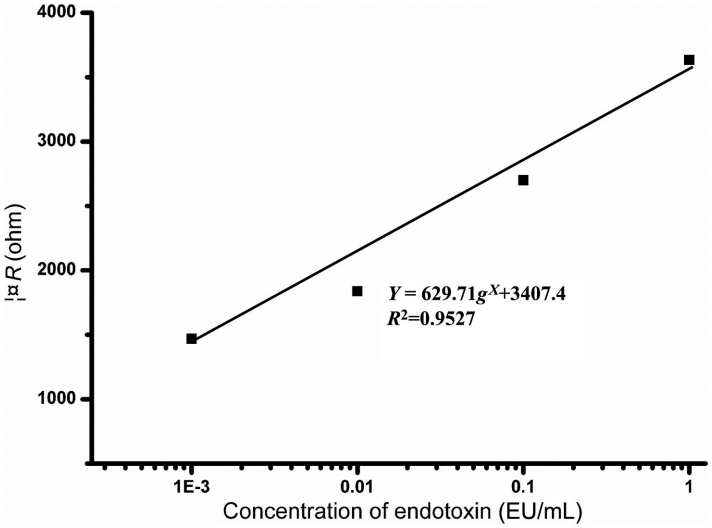

FIG. 7 *The linear relationship between the change of resistance (∆R) of the biosensor and the logarithmic value of endotoxin concentration. Endotoxin concentrations were as follows: 0.001, 0.01, 0.1, 1 EU/mL.*

the main ingredient of endotoxin is lipopolysaccharides, BSA was chosen as possible interfering substance in order to evaluate the selectivity of the biosensor. The biosensor was also incubated in endotoxin samples containing 500 ng/mL BSA, which did not cause the EIS data to change (Fig. 6). This is the potential advantage of choosing the aptamer as a biological element. The prepared biosensor was used to detect different concentrations of endotoxin in pyrogen-free water. In the range of 0.001–1 EU/mL, the increase in surface resistance of the biosensor was linear with the logarithmic value of the endotoxin concentration. The linear regression equation was $y = 629.7\lg^X + 3407.4$ with $R^2 = 0.9527$ (Fig. 7). The biosensor showed a low detection limit (0.001 EU/mL), indicating that the optimized biosensor was expected to be used for detection of endotoxin in biological products.

4. Conclusions

We developed a biosensor that used an original high-affinity aptamer EAQ3 to detect endotoxin. Biolayer interferometry was used to measure the aptamer–LPS interactions. The EAQ3–LPS interaction had a K_D of 22.9 nM, so EAQ3 was chosen as the biosensor element. A biosensor was successfully constructed by immobilizing amino-modified aptamers on a gold electrode surface using MPA as a linker. The biosensor displayed a high affinity for detection of endotoxin and a low detection limit (0.001 EU/mL), along with a good linear relationship in the endotoxin concentration range of 0.001–1 EU/mL. We believe that after optimization, this biosensor will be useful for detecting endotoxin in practical applications.

5. Author Contributions

GuoQing Ying and ShuQing Chen conceived and designed the experiments; GuoQing Ying and MinJun Wang performed the experiments; GuoQing Ying, MinJun Wang, Yu Yi, JianShu Chen, JianFeng Mei, and YanLu Zhang analyzed the data; GuoQing Ying and ShuQing Chen contributed materials and analysis tools; GuoQing Ying and MinJun Wang wrote the paper. GuoQing Ying and ShuQing Chen agreed with the final approval of the version to be published.

Declaration of Interest. The authors declare no conflict of interest.

6. References

[1] Anwar M. A, and Choi S. (2014). Marine Drugs 12(5), 2483–2485.
[2] Kim, Y. G., Lee, C. S., Chung, W. J., Kim, E. M., Shin, D. S., Rhim, J. H., Lee, Y. S., and Kim, B. G. (2005). Biochem. Biophys. Res. Commun. 329(1), 312–317.
[3] Iwanaga S. (2007). Proc. Jap. Acad. 83(4), 108–110.
[4] Tuerk, C., and Goldberg, L. (1990). Science, 249, 505–510.
[5] Citartan, M., Gopinath, S. C., Tominaga, J., Tan, S. C., and Tang, T. H. (2012). Biosens. Bioelectron. 34(1), 1–11.
[6] He, F., Tang, Y., Wang, S., Li, Y., and Zhu, D. (2005). J. Am. Chem. Soc. 127(35), 109–129.
[7] Liu, J., Lee, J. H., and Lu, Y. (2007). Anal. Chemis. 79(11), 412–415.
[8] Ronkainen, N. J., Halsall, H. B., and Heineman, W. R. (2010). Electrochemical biosensors. Chem Soc Rev. 39(5), 1747–1763.
[9] Ma, X. Y., Jiang, Y. H., and Jia, F. (2014). J. Microbiol. Methods. 98(1), 94–98.
[10] Alhadrami, H., Chinnappan, R., Eissa, S., Rahamn, A. A., and Zourob, M. (2017). Anal. Biochem. 525, 78–84.
[11] Zuzuarregui, A., Souto, D., Pérezlorenzo, E., Arizti, F., Sánchez-Gómez, S. Tejada, M. G., Brandenburg, K., Arana, S., and Mujika, M. (2015). Analyst 140(2), 654–660.
[12] Ying, G. Q., Zhu, F. F., Yi, Y., Chen, J. S., Mei, J. F., Zhang, Y. L., and Chen, S. Q. (2015). Biotechnol. Lett. 37(8), 1601–1605.
[13] Berezovski, M., Drabovich, A., Krylova, S. M., Musheev, M., Okhonin, V., Petrov, A., and Krylov, S. N. (2005). J. Am. Chem. Soc. 127(9), 3165–3171.
[14] Geddes, N. J., Paschinger, E. M., Furlong, D. N., Caruso, F., Hoffmann, C. L., and Rabolt, J. F. (1995). Thin Solid Films 260(2), 192–199.
[15] Brett, C. M. A., Kresak, S., Hianik, T., and Brett, A. M. O. (2003). Electroanalysis 15(5–6), 557–565.
[16] Su, W., Nguyen, H. T., Cho, M., Son, Y., and Lee, Y. (2010). Synth. Met. 160(23–24), 2471–2475.
[17] Cai, H., Lee, T. M. H., and Hsing, I. M. (2006). Sens. Actuators B Chem. 114(1), 433–437.